



Published in final edited form as:

Oncogene. 2017 April ; 36(15): 2184–2190. doi:10.1038/onc.2016.361.

Mechanistic Validation of a Clinical Lead Stapled Peptide that Reactivates p53 by Dual HDM2 and HDMX Targeting

Franziska Wachter¹, Ann M. Morgan¹, Marina Godes¹, Rida Mourtada^{1,2}, Gregory H. Bird¹, and Loren D. Walensky^{1,*}

¹Department of Pediatric Oncology and the Linde Program in Cancer Chemical Biology, Dana-Farber Cancer Institute, Boston, MA

²The Harvard-MIT Program in Health Sciences and Technology, Massachusetts Institute of Technology, Cambridge, MA

Abstract

Hydrocarbon-stapled peptides that display key residues of the p53 transactivation domain have emerged as bona fide clinical candidates for reactivating the tumor suppression function of p53 in cancer by dual targeting of the negative regulators HDM2 and HDMX. A recent study questioned the mechanistic specificity of such stapled peptides based on interrogating their capacity to disrupt p53/HDM2 and p53/HDMX complexes in living cells using a new recombinase enhanced bimolecular luciferase complementation platform (ReBiL). Here, we directly evaluate the cellular uptake, intracellular targeting selectivity, and p53-dependent cytotoxicity of the clinical prototype ATSP-7041. We find that under standard serum-containing tissue culture conditions, ATSP-7041 achieves intracellular access without membrane disruption, dose-dependently dissociates both p53/HDM2 and p53/HDMX complexes but not an unrelated protein complex in long-term ReBiL experiments, and is selectively cytotoxic to cancer cells bearing wild-type p53 by inducing a surge in p53 protein level. These studies underscore the importance of a thorough step-wise approach, including consideration of the time-dependence of cellular uptake and intracellular distribution, in evaluating and advancing stapled peptides for clinical translation.

INTRODUCTION

Helix-in-groove protein interactions represent the structural basis for a host of signaling mechanisms implicated in human disease^{1, 2}. Among the most established and clinically-relevant interactions are the complexes between the alpha-helical transactivation domain of p53 and its negative regulators HDM2 and HDMX³. p53 is an essential tumor suppressor that is frequently mutated in human cancer to avoid cell cycle arrest or apoptosis in response to DNA damage⁴. Alternative oncogenic mechanisms for p53 suppression in cancer involve the overexpression of HDM2, an E3 ligase that binds, inhibits, and destroys p53⁵, and HDMX, which lacks E3 ligase activity and instead binds and sequesters p53, and may

Users may view, print, copy, and download text and data-mine the content in such documents, for the purposes of academic research, subject always to the full Conditions of use: http://www.nature.com/authors/editorial_policies/license.html#terms

*Correspondence: Loren D. Walensky, MD, PhD, Dana-Farber Cancer Institute, 450 Brookline Avenue, LC3216, Boston, MA 02215, Loren_Walensky@dfci.harvard.edu.

enhance HDM2 function through heterodimeric interaction⁶. When HDM2 and HDMX are overproduced, cancer cells are under less genetic pressure to mutate p53, since the tumor suppressor protein is otherwise neutralized. Thus, in the context of cancers bearing wild-type p53, inhibitors of HDM2 and HDMX have the potential to restore p53 activity, prompting vigorous efforts to translate such strategies to the clinic.

The small molecule Nutlin-3a selectively blocks HDM2 and thereby produces a dramatic increase in cellular p53 protein⁷. In the absence of HDMX, such inhibitors restore p53-mediated apoptosis, justifying the advancement of next-generation analogs such as RO5045337 to clinical testing. However, in the presence of HDMX, the drug-induced surge in p53 can be ineffectual due to the rapid formation of inhibitory p53-HDMX complexes⁸. We previously developed a series of stapled peptides modeled after the α -helical p53 transactivation domain, which naturally engages both HDM2 and HDMX, and identified a lead (*i, i+7*) stapled construct with nanomolar binding affinity to both targets and the capacity to restore p53-dependent cell death *in vitro* and *in vivo*^{8,9}. Like many small molecule leads, a shortcoming of our prototype construct, SAH-p53-8, was its avid serum-binding activity, which limited its cellular potency and clinical advancement, prompting sequence-based optimization¹⁰. By retaining our original (*i, i+7*) staple position and the essential residues for HDM2/HDMX interaction (e.g. F19, W23), but sampling alternative residues based on phage display results, next-generation stapled p53 peptides with drug-like properties were developed¹⁰, one of which is currently being tested in clinical trials (ClinicalTrials.gov identifier: NCT02264613). Similar design variations on this theme have led other investigators to generate additional series of stapled p53 peptides that display varying degrees of biological activity, but none have advanced to clinical testing thus far^{11,12}.

An obvious requirement for on-mechanism biological function of stapled peptides is intracellular access for target engagement. The recent development of ReBiL, a split-luciferase system for probing intracellular protein targeting by small molecule and peptide ligands, provided a new opportunity to evaluate compounds reported to modulate the p53 pathway¹³. Several key conclusions of the study were that stapled peptides may not disrupt p53/HDM2 or p53/HDMX interactions efficiently in living cells and that cytotoxicity can be p53-independent if non-specific membrane disruption ensues. Given the conflicting interpretations of data regarding the biological activity and mechanism of action of stapled p53 peptides^{8,10,12,13}, coupled with the potentially confounding factors of having conducted ReBiL assays over short time courses and without direct measurement of cellular uptake, we undertook a step-wise approach to evaluating the mechanism of action of stapled p53 peptides in cellular systems.

RESULTS AND DISCUSSION

One of the challenges in cross-comparing the biochemical and biological activities of stapled p53 peptides generated by different laboratories is ensuring that all constructs are synthesized, purified, and quantitated in a uniform manner. Thus, we initiated our study by re-synthesizing an exemplary panel of stapled p53 peptides reported by distinct research groups, namely ATSP-7041¹⁰, SAH-p53-8⁸, and Staplin¹¹ (Figure 1a, Supplementary Figure

1). We generated the compounds according to our established methods^{14, 15}, using LC/MS-based purification and amino acid analysis for rigorous quantitation. To avoid any potentially confounding effects of exposing cells to serum-free treatments and to better simulate physiologic conditions required for clinical translation, all studies were performed with 10% serum. First, we conducted a cellular uptake assessment by exposing SAOS-2 parental cells (used to construct the ReBiL cell lines) to fluorescently-labeled stapled p53 peptides at a dose of 5 μ M for 4 hours in standard serum-containing media, followed by washing, trypsinization to remove any protein surface-bound peptide, repeat washing, cellular lysis, and FITC scan of electrophoresed lysates. We observed fluorescent signal in the lysates of cells treated with ATSP-7041 and its F19A mutant control, with FITC-Staplin peptide also detected, although at lower levels (Figure 1b). Consistent with our prior studies^{8, 9}, there is little to no FITC-SAH-p53-8 signal after cellular treatment for 4 hours in the presence of 10% fetal bovine serum (FBS). Next, we investigated whether the observed FITC signal in cellular lysates could have achieved intracellular access by direct membrane disruption. We performed LDH release assays on SAOS-2 cells 30 minutes after treating cells in standard serum-containing media with a serial dilution of peptides starting from 30 μ M, well above the 5 μ M dose used to assess cellular uptake. Importantly, no membrane disruption was observed for any of the stapled p53 peptides (Figure 1c). As another measure to rule-out non-specific activity, we tested the effect of stapled peptide treatments on the viability of p53-null SAOS-2 cells, which should exhibit no mechanism-based response to the compounds due to the absence of wild-type p53. Using a serial dilution starting at the same high micromolar dose of peptide applied in the LDH release assays, we found no evidence of non-specific cytotoxicity, as measured by viability assay at 72 hours (Figure 1d). By applying this sequence of screening assays, which in our view should be a prerequisite for cellular testing of stapled peptides in general¹⁶, we document effective cellular uptake of a subset of stapled p53 peptides under standard 10% serum conditions, and no evidence of membrane disruption or p53-independent toxicity for any of the compounds.

The ReBiL protein interaction assay system is ideally suited to measure the disruptive effect of small molecules and peptides on intracellular protein interactions¹³. In the context of evaluating p53/HDM2 and p53/HDMX complexes, the selected cell line of choice was SAOS-2, an osteosarcoma cell line that is itself p53-null to avoid any potentially confounding effects of p53-mediated cytotoxicity on the ReBiL signal⁸. For the same reason, a mutant p53 isoform (aa 2–312 truncate; R273H) was chosen for doxycycline-induced expression in the ReBiL system. In a previously reported study¹³, doxycycline induction of the protein complexes was performed first, followed by doxycycline withdrawal upon treating the cells with small molecules or stapled p53 peptides. Because the ReBiL signal declines on its own during the subsequent 6 hour assay period, so does the window for detecting specific compound activity. What's more, the mechanisms for cellular uptake of small molecules and stapled peptides are different, with the former being rapid diffusion and the latter time-dependent, fluid-phase macropinocytosis^{17, 18}. Thus, short-term ReBiL assays may not provide sufficient time for stapled peptides to emerge from pinosomes, transit to the cytoplasm and nucleus, and achieve appreciable extra-vesicular concentrations to exert biochemical activity. Despite this experimental design constraint, ATSP-7041 dose-

responsively disrupted pre-formed p53/HDM2 and p53/HDMX complexes in the prior study, but compound performance was deemed slow for HDM2 and marginal for HDMX¹³.

To eliminate the potentially confounding variables of a progressively fading ReBiL signal and time courses of limited duration, here we performed the ReBiL analyses upon co-treating with doxycycline and stapled peptides for 10 hour time periods. In addition, we used the unrelated protein interaction between BRCA1 and BARD1 as a negative control for ReBiL testing. For Nutlin-3a, the small molecule positive control for selective HDM2 inhibition, we observed effective blockade of the p53-HDM2 interaction, but no activity against p53/HDMX or BRCA1/BARD1 (Figure 2a–c). In contrast, ATSP-7041 exhibited dose-responsive disruption of both the p53-HDM2 and p53-HDMX interactions, with no disruptive effect on BRCA1/BARD1 complex formation (Figure 2d–f). ATSP-7342, the F19A point mutant of ATSP-7041, had no effect on any of the ReBiL cell lines (Figure 2g–i). SAH-p53-8, whose uptake is impeded by 10% serum conditions, showed modest activity against the p53-HDM2 and p53-HDMX interactions at the higher 20 μ M dose level with no effect on BRCA1/BARD1 (Figure 2j–l), whereas Staplin disrupted only the p53/HDM2 interaction (in non-dose-responsive fashion), with no effect on p53/HDMX or BRCA1/BARD1 (Figure 2m–o). Based on these data, ATSP-7041 indeed represents an optimized version of SAH-p53-8, and effectively disrupts intracellular p53/HDM2 and p53/HDMX complexes in a dose-responsive and sequence-dependent manner over time.

To link the demonstrated on-mechanism biochemical activity of ATSP-7041 in ReBiL cells to p53-mediated killing of cancer cells, we performed viability testing and correlative p53 western blotting of SJS-A-1 (HDM2-dependent) and SJS-A-X (HDM2- and HDMX-dependent) osteosarcoma cells bearing wild-type p53. Whereas Nutlin-3a selectively impaired the viability of SJS-A-1 cell lines, ATSP-7041, but not its F19A point mutant, killed both SJS-A-1 and SJS-A-X lines in the presence of 10% serum (Figure 3a–b). Under these same conditions, SAH-p53-8 had little (SJS-A-1) to no (SJS-A-X) effect, whereas Staplin was inactive in both cell lines except for precipitous toxicity at the highest dose level (30 μ M) in SJS-A-1 cells (Supplementary Figure 2a–b). Importantly, we found that treatment of SJS-A-1 and SJS-A-X cells with ATSP-7041 produced an increase in p53 protein levels, which was not observed upon treatment with ATSP-7342 (Figure 3c). These viability and p53 western data are consistent with the previously reported effects of ATSP-7041 on SJS-A-1 cells, including (1) upregulation of p53 protein and the resultant increased expression of p21, as assessed at the RNA and protein levels; (2) cell cycle arrest, apoptosis induction, and reduced cell viability, as assessed by BrdU, annexin V binding, and MTT assays, respectively; and (3) tumor suppression in an *in vivo* xenograft model of SJS-A-1 osteosarcoma¹⁰.

Confocal microscopy confirmed that FITC-ATSP peptides were initially localized to intracellular vesicles (Figures 3d and e). Over the 4 hour time course, the cytosolic and especially nuclear accumulation of ATSP-7041 became progressively evident, whereas ATSP-7342, which does not target HDM2 or HDMX, showed no nuclear accumulation (Figure 3d–e and Supplementary Figure 3). These data reinforce the importance of establishing the cellular uptake kinetics and cellular distribution of stapled peptides in advance of designing experiments to test phenotypic endpoints, as highlighted by the time

required for ATSP-7041 to achieve the requisite cellular localization to exert functional activity.

p53 is a “clear and present danger” to the development, maintenance, and chemoresistance of human cancer. As such, the majority of cancer cells disarm p53 by deletion, mutation, degradation, and/or sequestration^{5, 19–21}. When the risk of wild-type p53 is mitigated in cancer cells by HDM2 and/or HDMX overexpression, targeted inhibition of these negative regulators holds promise to restore p53-mediated cell death. To date, the two drug modalities that have advanced to clinical testing are selective small molecule HDM2 inhibitors (RO5045337, Roche and AMG233, Amgen) and dual HDM2/HDMX targeting stapled p53 peptides (ALRN-6924, Aileron Therapeutics). The latter approach has the added benefit of overcoming HDMX-mediated resistance to small molecule HDM2 inhibitors in the context of HDMX overexpression^{8, 10}, as demonstrated here by the differential effects of Nutlin-3a and ATSP-7041 in SJS-A-1 vs. SJS-A-X cell lines. Because stapled peptides represent a new drug modality with potential broad application to targeting pathologic helix-in-groove interactions¹⁶, intensive efforts have been underway to more fully understand their biophysical, biological, and pharmacokinetic properties.

In this context, one report claimed that a stapled peptide modeled after the pro-apoptotic BIM protein^{22, 23} exhibited no biological activity due to lack of cell penetrance²⁴, and another suggested that stapled peptides modeled after the p53 transactivation domain^{8, 9} were either nonspecific (although the data actually showed inactivity due to added serum)¹² or achieved cytotoxicity, at least in part, as a result of nonspecific membrane disruption¹³. In each of these cases, no direct measures of cellular uptake were performed and thus interpretations about stapled peptide performance were inferred rather than fully examined, leading to questionable conclusions and residual ambiguity. Given the importance of clarifying the intracellular mechanism of action that formed the basis for the first clinical trial of a stapled peptide in human cancer, we established a step-wise vetting workflow for ATSP-7041. Head-to-head comparison of uniformly synthesized and quantitated constructs across LDH release, cellular uptake, and non-specific cytotoxicity assay screening under standard serum-containing conditions demonstrated that stapled p53 peptides can unequivocally gain intracellular access without membrane disruption and without triggering non-specific cytotoxicity in the presence of standard 10% serum. The use of ReBiL, a highly sensitive and specific protein interaction cell assay system¹³, further confirmed the unique capacity of ATSP-7041 to disrupt both p53/HDM2 and p53/HDMX complexes in a dose-responsive, sequence-dependent, and protein interaction-specific fashion. Based on this rigorous mechanistic validation, ATSP-7041 was then tested in isogenic cell lines driven by HDM2 or HDM2/HDMX and was, again, the only construct to impair cellular viability in both contexts and in the presence of 10% serum. Importantly, ATSP-7041 killing coincided with upregulation of p53 and had no effect on p53-null cells. Thus, these data highlight the capacity to generate, validate, and clinically translate stapled peptides for intracellular targeting of pathologic protein interactions by applying a comprehensive step-wise workflow that spans structure-based design, chemical synthesis, biochemical testing, cellular uptake analysis, and validation of intracellular mechanism of action.

Supplementary Material

Refer to Web version on PubMed Central for supplementary material.

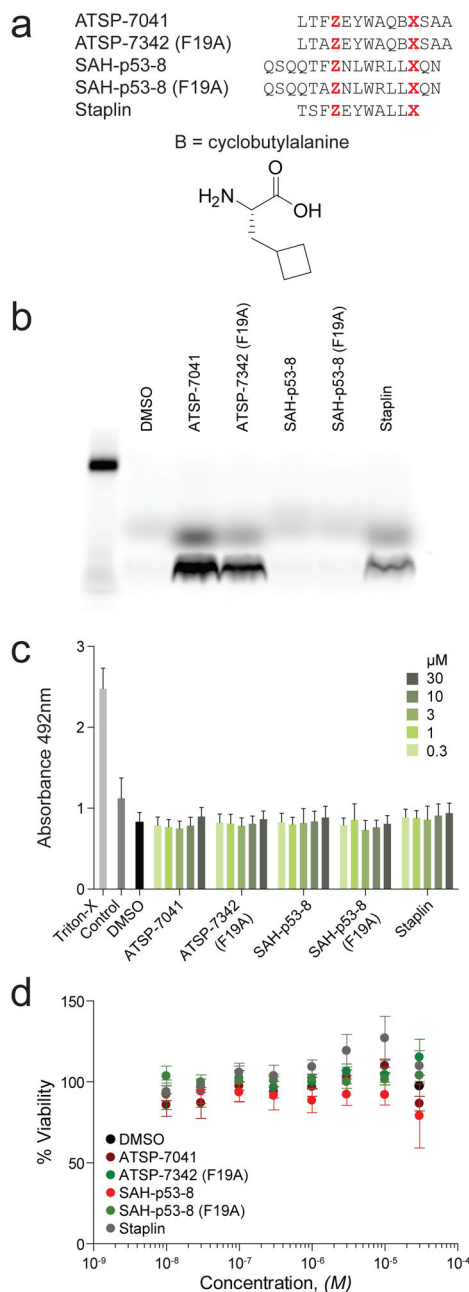
Acknowledgments

We thank E. Smith for graphical assistance, Lisa Cameron for assistance with confocal microscopy, and Alexandra Zoraian and Katherine Franklin for technical support. We appreciate the generosity of Drs. Y. Li and G. Wahl for providing the ReBiL cells for this study, hosting F.W. in their laboratory to conduct confirmatory experiments, and for helpful feedback on the manuscript. This work was supported by a Hyundai Hope on Wheels Quantum Award, Alex's Lemonade Stand Reach Grant, the Todd J. Schwartz Memorial Fund, and Leukemia and Lymphoma SCOR and Scholar Awards to L.D.W. F.W. is supported by an Alexander von Humboldt Foundation Feodor Lynen Fellowship, A.M.M. by NIH training grant T32GM007753, R.M. by Doctoral Foreign Studies Award DFS-134963 from the Canadian Institutes of Health Research, and A.Z. and K.F. by the William Lawrence and Blanche Hughes Foundation and a generous gift from Jim and Lisa LaTorre, respectively.

References

1. Kussie PH, Gorina S, Marechal V, Elenbaas B, Moreau J, Levine AJ, et al. Structure of the MDM2 oncoprotein bound to the p53 tumor suppressor transactivation domain. *Science*. 1996; 274:948–953. [PubMed: 8875929]
2. Sattler M, Liang H, Nettlesheim D, Meadows RP, Harlan JE, Eberstadt M, et al. Structure of Bcl-xL-Bak peptide complex: recognition between regulators of apoptosis. *Science*. 1997; 275:983–986. [PubMed: 9020082]
3. Wade M, Li YC, Wahl GM. MDM2, MDMX and p53 in oncogenesis and cancer therapy. *Nat Rev Cancer*. 2013; 13:83–96. [PubMed: 23303139]
4. Vousden KH, Lane DP. p53 in health and disease. *Nat Rev Mol Cell Biol*. 2007; 8:275–283. [PubMed: 17380161]
5. Honda R, Tanaka H, Yasuda H. Oncoprotein MDM2 is a ubiquitin ligase E3 for tumor suppressor p53. *FEBS Lett*. 1997; 420:25–27. [PubMed: 9450543]
6. Shvarts A, Steegenga WT, Riteco N, van Laar T, Dekker P, Bazuine M, et al. MDMX: a novel p53-binding protein with some functional properties of MDM2. *EMBO J*. 1996; 15:5349–5357. [PubMed: 8895579]
7. Vassilev LT, Vu BT, Graves B, Carvajal D, Podlaski F, Filipovic Z, et al. In vivo activation of the p53 pathway by small-molecule antagonists of MDM2. *Science*. 2004; 303:844–848. [PubMed: 14704432]
8. Bernal F, Wade M, Godes M, Davis TN, Whitehead DG, Kung AL, et al. A stapled p53 helix overcomes HDMX-mediated suppression of p53. *Cancer Cell*. 2010; 18:411–422. [PubMed: 21075307]
9. Bernal F, Tyler AF, Korsmeyer SJ, Walensky LD, Verdine GL. Reactivation of the p53 tumor suppressor pathway by a stapled p53 peptide. *J Am Chem Soc*. 2007; 129:2456–2457. [PubMed: 17284038]
10. Chang YS, Graves B, Guerlavais V, Tovar C, Packman K, To KH, et al. Stapled alpha-helical peptide drug development: a potent dual inhibitor of MDM2 and MDMX for p53-dependent cancer therapy. *Proc Natl Acad Sci U S A*. 2013; 110:E3445–3454. [PubMed: 23946421]
11. Tan BX, Brown CJ, Ferrer FJ, Yuen TY, Quah ST, Chan BH, et al. Assessing the Efficacy of Mdm2/Mdm4-Inhibiting Stapled Peptides Using Cellular Thermal Shift Assays. *Sci Rep*. 2015; 5:12116. [PubMed: 26159518]
12. Brown CJ, Quah ST, Jong J, Goh AM, Chiam PC, Khoo KH, et al. Stapled peptides with improved potency and specificity that activate p53. *ACS Chem Biol*. 2013; 8:506–512. [PubMed: 23214419]
13. Li YC, Rodewald LW, Hoppmann C, Wong ET, Lebreton S, Safar P, et al. A versatile platform to analyze low-affinity and transient protein-protein interactions in living cells in real time. *Cell Rep*. 2014; 9:1946–1958. [PubMed: 25464845]
14. Bird GH, Bernal F, Pitter K, Walensky LD. Synthesis and biophysical characterization of stabilized alpha-helices of BCL-2 domains. *Methods Enzymol*. 2008; 446:369–386. [PubMed: 18603134]

15. Bird GH, Crannell WC, Walensky LD. Chemical synthesis of hydrocarbon-stapled peptides for protein interaction research and therapeutic targeting. *Curr Protoc Chem Biol.* 2011; 3:99–117. [PubMed: 23801563]
16. Walensky LD, Bird GH. Hydrocarbon-stapled peptides: principles, practice, and progress. *J Med Chem.* 2014; 57:6275–6288. [PubMed: 24601557]
17. Edwards AL, Wachter F, Lammert M, Huhn AJ, Luccarelli J, Bird GH, et al. Cellular Uptake and Ultrastructural Localization Underlie the Pro-apoptotic Activity of a Hydrocarbon-stapled BIM BH3 Peptide. *ACS Chem Biol.* 2015; 10:2149–2157. [PubMed: 26151238]
18. Walensky LD, Kung AL, Escher I, Malia TJ, Barbuto S, Wright RD, et al. Activation of apoptosis in vivo by a hydrocarbon-stapled BH3 helix. *Science.* 2004; 305:1466–1470. [PubMed: 15353804]
19. Baker SJ, Fearon ER, Nigro JM, Hamilton SR, Preisinger AC, Jessup JM, et al. Chromosome 17 deletions and p53 gene mutations in colorectal carcinomas. *Science.* 1989; 244:217–221. [PubMed: 2649981]
20. Moll UM, LaQuaglia M, Benard J, Riou G. Wild-type p53 protein undergoes cytoplasmic sequestration in undifferentiated neuroblastomas but not in differentiated tumors. *Proc Natl Acad Sci U S A.* 1995; 92:4407–4411. [PubMed: 7753819]
21. Nigro JM, Baker SJ, Preisinger AC, Jessup JM, Hostetter R, Cleary K, et al. Mutations in the p53 gene occur in diverse human tumour types. *Nature.* 1989; 342:705–708. [PubMed: 2531845]
22. Bird GH, Gavathiotis E, LaBelle JL, Katz SG, Walensky LD. Distinct BimBH3 (BimSAHB) stapled peptides for structural and cellular studies. *ACS Chem Biol.* 2014; 9:831–837. [PubMed: 24358963]
23. LaBelle JL, Katz SG, Bird GH, Gavathiotis E, Stewart ML, Lawrence C, et al. A stapled BIM peptide overcomes apoptotic resistance in hematologic cancers. *J Clin Invest.* 2012; 122:2018–2031. [PubMed: 22622039]
24. Okamoto T, Zobel K, Fedorova A, Quan C, Yang H, Fairbrother WJ, et al. Stabilizing the pro-apoptotic BimBH3 helix (BimSAHB) does not necessarily enhance affinity or biological activity. *ACS Chem Biol.* 2013; 8:297–302. [PubMed: 23151250]
25. Li M, Brooks CL, Wu-Baer F, Chen D, Baer R, Gu W. Mono- versus polyubiquitination: differential control of p53 fate by Mdm2. *Science.* 2003; 302:1972–1975. [PubMed: 14671306]

**Figure 1.**

Step-wise screening of stapled p53 peptides for cellular uptake, membrane disruption and p53-independent cytotoxicity. **(a)** Sequence composition of a series of reported stapled p53 peptides. Hydrocarbon-stapled peptides corresponding to the α -helical transactivation domain of p53 were synthesized, N-terminally derivatized with acetyl or FITC- β Ala, purified, and quantitated by amino acid analysis using our established methods^{14, 15}. Fmoc-cyclobutylalanine was purchased from Chem-Impex. Stapled peptide compositions, their observed masses, and use by figure are tabulated in Supplementary Table 1. **(b)** Level of intracellular FITC-labeled stapled peptides, as detected by FITC scan of electrophoresed

lysates of treated parental SAOS-2 cells. SAOS-2 cells (ATCC, verified mycoplasma-free using the MycoAlert™ mycoplasma detection kit [Lonza Biologicals, Inc.]) were seeded in 6-well plates (2.5×10^5 cells/well) in DMEM containing 10% FBS and, after overnight incubation, treated with 5 μ M peptide or vehicle (0.3% DMSO) for 4 hours. After 4 hours, the cells were washed with PBS, trypsinized for 10 min, washed twice more, lysed (1% CHAPS, 150 mM NaCl, 20 mM TRIS, pH 7.2), and lysates subjected to SDS PAGE electrophoresis and FITC scan (Typhoon TM FLA 9500 Biomolecular Imager, GE Healthcare Life Sciences). (c) Quantitation of LDH release from SAOS-2 cells treated in 10% serum with a serial dilution of stapled p53 peptide (30 μ M starting dose), as compared to untreated, vehicle-treated (0.3% DMSO), and Triton X-100 (1%) exposed cells. SAOS-2 cells were plated in 96-well format (2×10^4 cells/well) in DMEM containing 10% FBS. On the following day, the cells were treated with the indicated concentrations of peptide and LDH release was detected using the LDH Cytotoxicity Detection Kit (Roche) according to the manufacturer's instructions. Error bars are mean \pm s.e.m for experiments performed in technical duplicate and repeated three times with independent cell plating and treatments. (d) Cell viability of SAOS-2 cells (p53-null) treated in 10% serum with a serial dilution of stapled p53 peptides, as measured by CellTiter-Glo assay. SAOS-2 (p53-null) cells were plated in 96-well opaque plates (7.5×10^3 /well) in DMEM containing 10% FBS and, the following day, the cells were treated with the indicated concentrations of peptide or vehicle control (0.3% DMSO). Peptide stocks (10, 3.3, 1.1, 0.33, 0.11, 0.03, 0.01 mM in 100% DMSO) were diluted into ddH₂O to achieve 10X working stocks of 300, 100, 30, 10, 3, 1, 0.3 and 0.1 μ M, which were then diluted 10-fold into the treatment wells. Cell viability was measured after 72 hours by CellTiter-Glo assay (Promega), performed according to the manufacturer's instructions, and percent viability calculated based on the untreated controls. Error bars are mean \pm s.e.m for experiments performed in technical duplicate and repeated three times with independent cell plating and treatments.

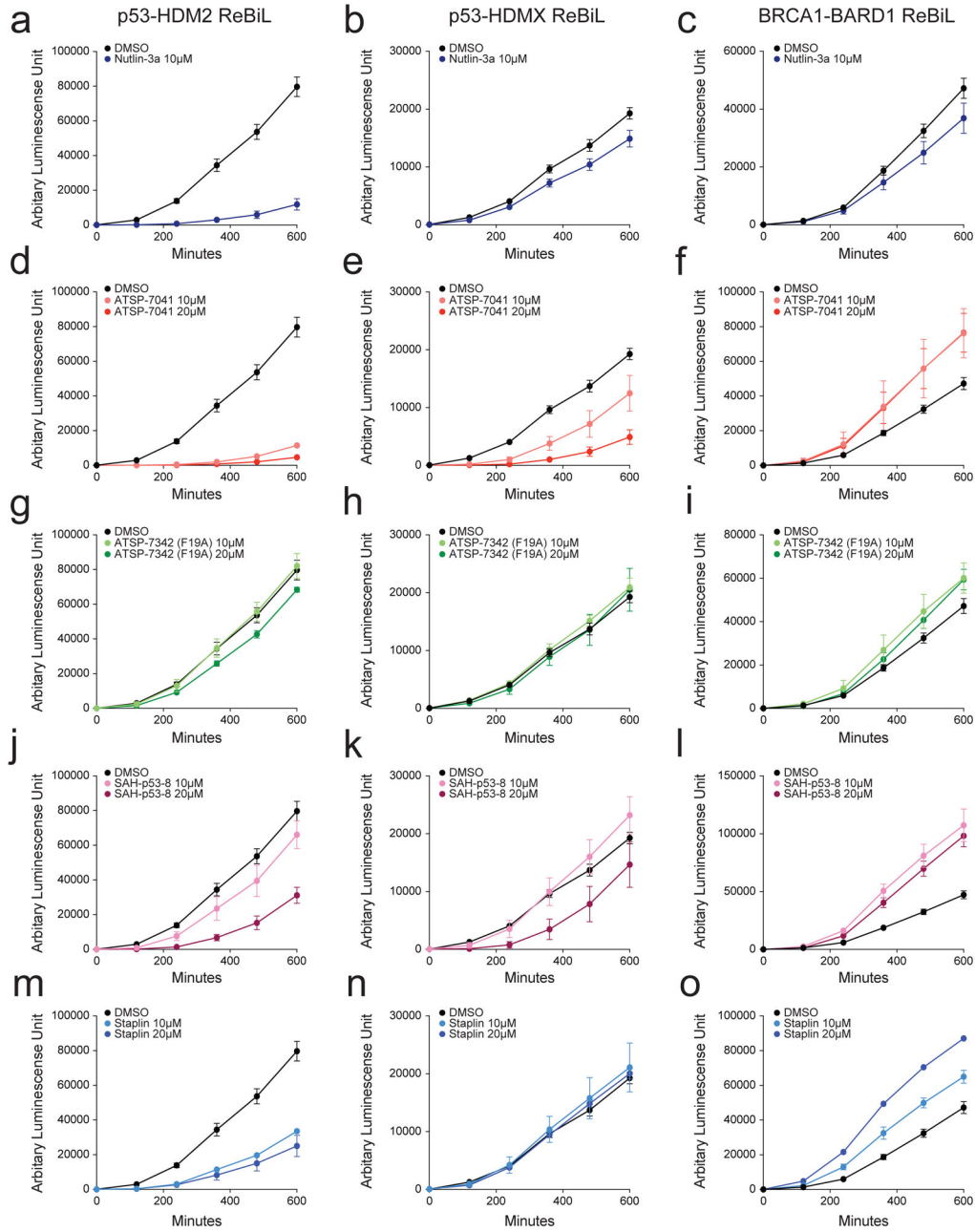


Figure 2.

Evaluation of specific, intracellular protein interaction disruption using the ReBiL assay platform. Effect of Nutlin-3a (a–c), ATSP-7041 (d–f), ATSP-7342 (g–i), SAH-p53-8 (j–l), and Staplin (m–o) on the ReBiL luminescence signal generated by SAOS-2 cells co-expressing p53/HDM2 (left), p53/HDMX (middle) or BRCA1/BARD1 (right) in the presence of doxycycline and 10% serum. SAOS-2 ReBiL cells (Wahl laboratory, verified mycoplasma-free using the MycoAlert™ mycoplasma detection kit [Lonza Biologics, Inc.]), were plated in 96-well opaque plates (2×10^4 cells/well) and incubated overnight at 37°C in DMEM/F12 media (50:50) containing FBS (10%), G418 (400 µg/mL), and ciprofloxacin

(10 µg/ml). The following day, doxycycline (500 ng/ml; Sigma-Aldrich), D-luciferin potassium salt (100 µM; L-8220, Biosynth), and the indicated concentration of small molecule or peptide were added. Of note, Nutlin-3a dosing was not escalated above 10 µM due to the emergence of nonspecific activity, as reflected by a similar level of signal suppression in both the p53/HDMX and BRCA1/BARD1 cell lines where no mechanistic effect is expected. Luminescence was recorded every 2 hours on a BMG LABTECH CLARIOstar plate reader (integration time 0.8 s), with culture plates maintained in an incubator between measurements. Error bars are mean ± s.d. for experiments performed in technical triplicate for p53/HDM2 and p53/HDMX ReBiL, and technical duplicate for the negative control BRCA1/BARD1. The experiments were performed in biological triplicate, each with independent ReBiL cell platings and treatments.

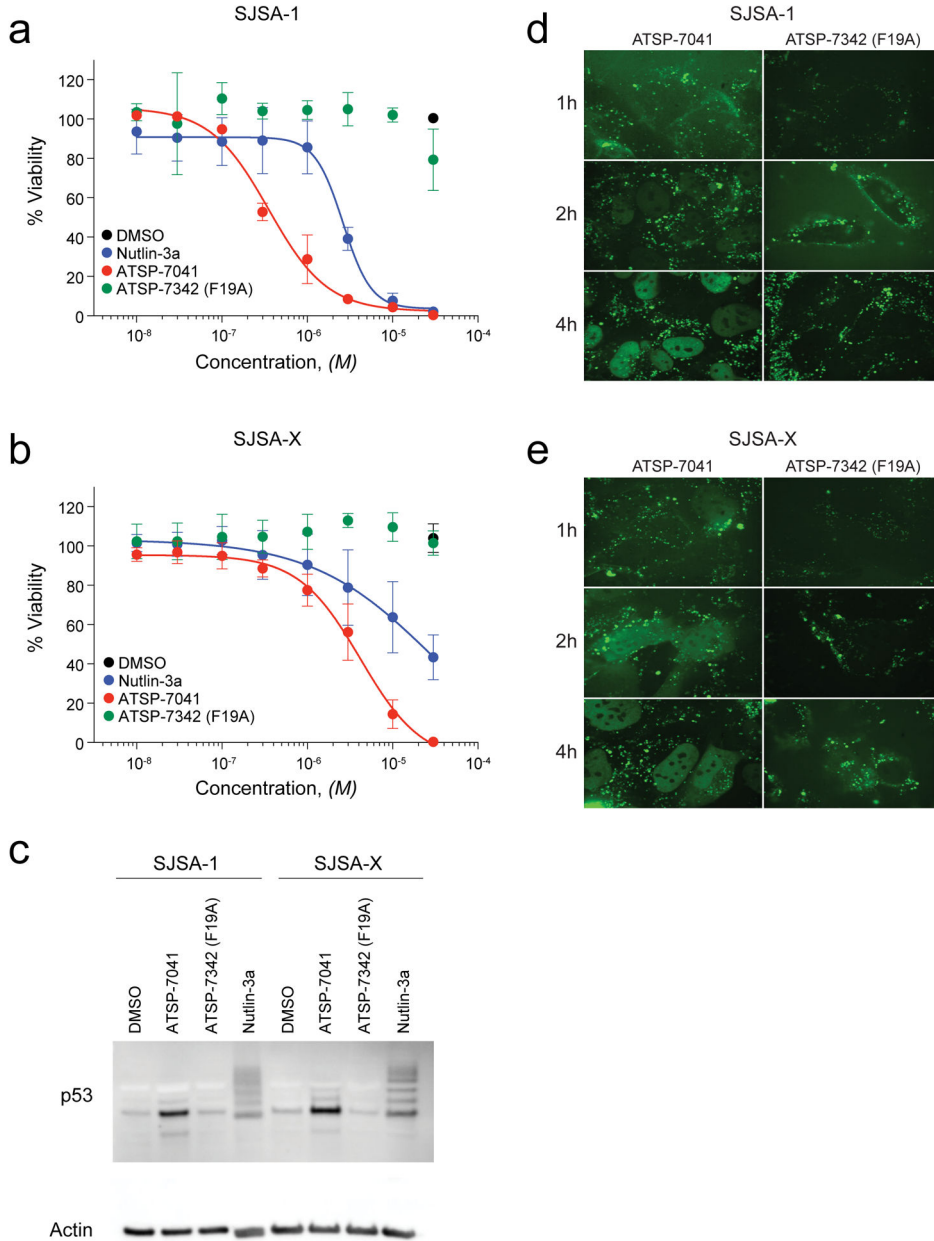


Figure 3. Differential effects of Nutlin-3a and ATSP-7041 on isogenic SJSA cell lines dependent on either HDM2 or HDM2/HDMX. **(a–b)** Cell viability responses of SJSA-1 **(a)** and SJSA-X **(b)** cells to treatment with Nutlin-3a, ATSP-7041, or ATSP-7342 in the presence of 10% serum, as evaluated by CellTiter-Glo assay. SJSA-1 and SJSA-X cells (Wahl laboratory, verified mycoplasma-free using the MycoAlert™ mycoplasma detection kit [Lonza Biologics, Inc.]) were plated in 96-well opaque plates (7.5×10^3 /well) in DMEM containing 10% FBS and, the following day, the cells were treated with the indicated concentrations of peptide or vehicle control (0.3% DMSO). Peptide stocks (10, 3.3, 1.1, 0.33, 0.11, 0.03, 0.01

mM in 100% DMSO) were diluted into ddH₂O to achieve 10X working stocks of 300, 100, 30, 10, 3, 1, 0.3 and 0.1 μ M, which were then diluted 10-fold into the treatment wells. Cell viability was measured after 72 hours by CellTiter-Glo assay (Promega), performed according to manufacturer's instructions, and percent viability calculated based on the untreated controls. Error bars are mean \pm s.e.m. for experiments performed in technical duplicate and repeated three times with independent cell plating and treatments. (c) p53 western blot analysis of electrophoresed lysates from SJSA-1 and SJSA-X cells treated for 8 hours with Nutlin-3a, ATSP-7041, or ATSP-7342 in the presence of 10% serum. The series of p53-immunoreactive bands that run above p53, and most evident in the Nutlin-3a lanes, are consistent with HDM2-ubiquitylated species, as reported²⁵. SJSA-1 and SJSA-X cells were plated in 6-well plates (2×10^5 /well) overnight in DMEM containing 10% FBS and, the following day, the cells were treated with 10 μ M peptide or vehicle control (0.1% DMSO) in 10% FBS-containing media for 8 hours. The cells were then collected, washed, lysed (1% CHAPs, 150 mM NaCl, 20mM TRIS, pH 7.2) and the crude lysates cleared by centrifugation. The concentration of protein in the supernatant was determined using the Pierce BCA assay (Thermo Fisher). A 10 μ g aliquot of protein from each condition was electrophoresed on a 4–12% Bis-Tris polyacrylamide gel (Invitrogen) and western blotting performed with p53 (DO-1: sc-126, Santa Cruz Biotechnology) and β -actin (clone AC-15, Sigma-Aldrich) antibodies using Amersham ECL Prime Western Blotting Detection Reagent and an Amersham Imager 600. (d–e) Confocal microscopy images of SJSA-1 (d) and SJSA-X (e) cells treated with FITC-ATSP-7041 or FITC-ATSP-7342 in the presence of 10% serum. Cells were plated in 8-well glass chambers (2.5×10^4 cells/well) in DMEM containing 10% FBS. After 48 hours, the media was replaced with OptiMEM containing 10% FBS and treated with 5 μ M peptide. Confocal images were acquired at the indicated time points using a Yokogawa CSU-X1 spinning disk confocal (Andor Technology) mounted on a Nikon Ti-E inverted microscope (Nikon Instruments), equipped with a 100x 1.4 NA Plan Apo objective lens, Orca ER CCD camera (Hamamatsu Photonics), and 488 nm laser. Acquisition parameters, shutters, filter positions and focus were controlled by Andor iQ software (Andor Technology).